Computer Methods and Programs in Biomedicine 243 (2024) 107889

Contents lists available at ScienceDirect

Computer Methods and Programs in Biomedicine

journal homepage: www.elsevier.com/locate/cmpb

Endoscopic versus laparoscopic bariatric procedures: A computational biomechanical study through a patient-specific approach

Ilaria Toniolo [a,b], Paola Pirini [a], Silvana Perretta [c,d,e], Emanuele Luigi Carniel [b,f,*], Alice Berardo [a,b,g,*]

[a] Department of Civil, Environmental and Architectural Engineering, University of Padova, Italy
[b] Centre for Mechanics of Biological Materials, University of Padova, Italy
[c] IHU Strasbourg, Strasbourg, France
[d] IRCAD France, Strasbourg, France
[e] Department of Digestive and Endocrine Surgery, NHC, Strasbourg, France
[f] Department of Industrial Engineering, University of Padova, Italy
[g] Department of Biomedical Sciences, University of Padova, Italy

ARTICLE INFO

Keywords:
Computational biomechanics: Personalised medicine
Bariatric surgery
Clinical engineering
Endoscopic sleeve gastroplasty

ABSTRACT

Background and Objectives: Within the framework of computational biomechanics, finite element models of the gastric district could be seen as a potential clinical tool not only to study the effects apported by bariatric surgery, but also to compare different surgical techniques such as the new emerging Endoscopic Sleeve Gastroplasty (ESG) with respect to well-established ones (such as the Laparoscopic Sleeve Gastrectomy, LSG).
Methods: This work realized a fully computational comparison between the outcomes obtained from 10 patient-specific stomach models, which were used to simulate ESG, and the complementary results obtained from models representing the post-LSG of the same subjects. Specifically, once the ESG was simulated, a mechanical stimulus was applied by increasing an intragastric pressure up to a maximum of 5 kPa, in order to replicate the process of food intake, as well as for post-LSG models.
Results: : Results revealed non negligible differences between the techniques also within the same subject. In particular, not only LSG could lead to a greater reduction in the stomach volume (about 77 % at baseline, which is strictly linked to weight loss), but also influence the gastric distension (12 % less than pre-operative models). On the contrary, if ESG would be performed, a more similar pre-operative mechanical stimulation of the gastric walls may be seen (difference of about 1 %), thus preserving the mechanosensation, but the detriment of the volume reduction (about 56 % at baseline, and even decreases with increasing pressure). Moreover, since results suggested ESG may be more influenced by the pre-operative gastric cavity than LSG, a predictive model was proposed to support the surgical planning and the estimation of the volume reduction after ESG.
Conclusions: : ESG and LSG have substantial differences in their protocols and post-surgical effects. This work pointed out that variations between the two procedures may be observed also from a computational point of view, especially when including patient-specific geometries. These insights support gastric modelling as a valuable tool to evaluate, design and critically compare emerging bariatric surgical procedures, not only from empirical aspects and clinical outcomes, but also from a mechanical point of view.

1. Introduction

Computational biomechanics combines principles of engineering, medical science and biology to study the mechanical behaviour of biological systems, proposing an in-silico approach. From 1970, the rapid growth of computational power and the development of advanced numerical tools paved the way for the application of computational techniques to biomechanical problems and novel constitutive laws and codes were developed to describe the mechanical response of soft and hard tissues [1]. Thanks to Finite Element (FE) analysis, computational biomechanics has evolved significantly, spreading its application in a variety of clinical fields such as brain [2], heart and cardiovascular

* Corresponding authors at: Centre for Mechanics of Biological Materials, University of Padova, Italy.
E-mail addresses: emanueleluigi.carniel@unipd.it (E.L. Carniel), alice.berardo@unipd.it (A. Berardo).

https://doi.org/10.1016/j.cmpb.2023.107889
Received 10 July 2023; Received in revised form 25 October 2023; Accepted 25 October 2023
Available online 28 October 2023
0169-2607/© 2023 The Author(s). Published by Elsevier B.V. This is an open access article under the CC BY-NC-ND license (http://creativecommons.org/licenses/by-nc-nd/4.0/).

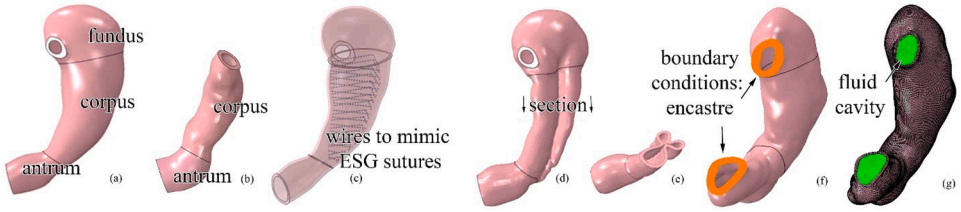

Fig. 1. Pre-surgical (a) and post-LSG (b) stomach models obtained from MRI segmentation. Example of the sutures pattern obtained by adding to pre-surgical models the wire features (c). Post-ESG stomach models after the wires' connector displacements (at 0.5 s of the simulation) (d) and section of the final shape of the post-ESG models (e). Representation of the boundary conditions (f) and fluid cavity on FE discretized model (g).

medicine [3,4], gastrointestinal [5,6], urinary [7] and musculoskeletal system [8,9], even at the cellular level [10]. One significant step forward has been the introduction of patient-specificity in computational models, by means of the use of medical imaging techniques, such as computed tomography (CT) [11] and magnetic resonance imaging (MRI), even supported by machine learning and artificial intelligence to enhance the accuracy in the model geometry [12,13]. The customisation provides an accurate representation of individual anatomy and possibly tissue properties, in order to predict the outcomes of different treatments and/or guide to the identification of optimal surgical strategies for the single patient [14–19].

The stomach, coupled with bariatric computational modelling, is an emerging field of biomechanics that has demonstrated its potential to deeply analyse several gastric issues, such as gastrooesophageal reflux disease and the implications/effects reported by bariatric surgery in terms of stomach mechanical response and gastric wall solicitation [20–23]. A strong and reliable biomechanical characterisation merged with FE analysis could be a valuable and powerful clinical tool, permitting not only a priori evaluation of new surgical procedures and instruments but also comparing existing bariatric interventions, e.g., the Endoscopic Sleeve Gastroplasty (ESG) and the Laparoscopic Sleeve Gastrectomy (LSG), proposing innovative surgical design to avoid post-surgical side effects.

Gastric restrictive bariatric endoscopy techniques (as ESG) have gained standing in the arsenal of weight loss therapies because of their minimally invasive nature, reversibility, and applicability in patients otherwise ineligible for bariatric surgery, replacing the more dated laparoscopic procedures (as LSG). Since 2013, ESG has been spreading thanks to its safety, feasibility, repeatability, and potential for reversibility [24]. The volume of the stomach is potentially reduced up to 70 % through plication of the greater curvature of the stomach using an endoscopic suturing device. The outpatient procedure is performed under general anaesthesia, lasting typically 1 hour, after which discharge is possible the same day [25]. The basic mechanisms of action are gastric volume reduction and alteration of gastric peristalsis. It is an innovative imitation of the LSG, which consists of the same intervention, but it is performed laparoscopically and involves the removal of the excessive part of the stomach. For these reasons, the comparison of these two bariatric techniques is natural. Currently, LSG remains the most-performed bariatric procedure worldwide with 128,382 interventions (50.2 % of all bariatric procedures), according to Sixth IFSO Global Registry Report 2021 [26]. Indeed, LSG provides a superior weight loss, but may significantly affect Quality-of-Life score and result in worsening of gastrointestinal symptoms including GERD [27]. On the contrary, ESG has an increased safety at 6-months and 12-month follow-ups with respect to LSG, and patients reported significantly better results in the gastrointestinal symptoms subdomain and a positive impact on both Quality-of-Life and comorbidities [27,28], confirming this technique a promising less invasive bariatric endoscopic procedure, which could lead to greater patient acceptance earlier in their disease or at a younger age. However, little is known about possible risks of adverse events after more than two years of follow-up, due to the quite novel technique and the limited retrospective nature of the studies.

This being the case, a computational approach could help in shed light on the biomechanics of the stomach in the follow-up of these two bariatric procedures. In particular, a patient-specific approach for the gastric modelling could highlight the modification induced by bariatric surgery on stomach conformation, showing whether the surgery standardizes the geometry of the stomach or if the latter is linked to the initial morphology of the organ and/or changes due to eating behaviours, comorbidities, etc. of the patient. A recent work showed that the geometrical conformation of the stomach after LSG (32 Fr guiding tube) is still affected by high inter-sample variability and the mechanical behaviour of the stomach and strain distribution of the gastric wall following a simulated inflation process varied according to the model [14].

Thus, for the first time, in this paper the outcomes of two bariatric surgery techniques, LSG and ESG were compared in terms of mechanical strain reached after both surgeries, referring to the same pre-surgical patient-specific stomach models. Starting from pre- and post-surgical models of a cohort of 23 patients with morbid obesity and submitted to LSG (reported in a previous work [14]), on 10 pre-surgical stomachs the ESG surgery was computationally simulated, following the specific procedure usually performs by the surgeon. Then, the results were analysed with respect to the post-surgical LSG models. The initial volume of the stomach after LSG and ESG, the pressure-volume behaviour following the simulation of an inflation process, and the elongation strain distribution of the gastric wall were used to perform the comparison. Finally, a rationale for models prediction after ESG was proposed.

2. Methods

From the cohort of the 23 patients described in [14,29], a set of 10 pre-surgical models were randomly chosen to simulate the ESG. A number of 10 patients was considered a representative group for the topic in order to provide a suitable description of ESG and comparison with LSG, in agreement with common sample size reported in literature on patient-specific finite element models (e.g., a sample size of 3 to 7 models [17–19] down to even a single case study [30]).

The procedure to obtain the FE models of the stomachs starting from Magnetic Resonance Image (MRI) scans was fully reported in a previous work [14]. It basically consisted of a first manual segmentation of the organ from the MRIs, followed by the post-processing of the gastric region to generate a double-layer-thickness virtual solid model composed of mucosa layer and muscularis stratum. Each layer and gastric region presented a different constant thickness (0.9 and 1.2 mm in the fundus, 1.2 and 1.5 mm in the corpus, and 0.9 and 1.8 mm in the antrum, for the submucosa-mucosa and muscularis layer, respectively). Finally, the FE discretisation was performed with an unstructured mesh by means of linear hexahedral elements with enhanced hourglass control, resulting in models of about 175,000 elements and 75,000 nodes. Moreover, to obtain a suitable description of the gastric wall, the thickness of the two layers was discretized with at least 3 elements for the submucosa-mucosa and 3 elements for the muscularis stratum. All the stomach models were fixed by imposing null displacement and rotation

Table 1
Constitutive material parameters of stomach regions.

Region	Layer	C_1 [kPa]	α_1 [-]	C_4 [kPa]	α_4 [-]	C_6 [kPa]	α_6 [-]
Fundus	submucosa-mucosa	0.15	1.05	3.30	0.96	3.70	1.11
	muscolaris	0.15	1.05	5.20	0.68	7.10	0.70
Corpus	submucosa-mucosa	0.15	1.05	3.00	1.80	3.00	1.68
	muscolaris	0.15	1.05	10.09	0.24	9.70	0.23
Antrum	submucosa-mucosa	0.15	1.05	4.50	0.11	3.00	0.54
	muscolaris	0.15	1.05	3.01	0.39	4.50	0.54

to the upper and lower extremities of the stomach cavity, which corresponded to the gastroesophageal and gastroduodenal junctions (Fig. 1f).

The ESG simulation was obtained by means of wire features that simulated the sutures applied during the surgery. In detail, 6–7 pairs of stitches per stomach depending on the size and organ characteristics of each patient were applied to reduce gastric capacity, as suggested in clinical works [31,32]. The sutures were placed in the gastric region of the corpus, leaving the fundus and antrum regions untouched. All points of the wires were anchored to the nearest five nodes of the FE model located in the inner intragastric surface by means of a Multi-Point Constraint connector. To each wire, a connector displacement was imposed to collapse the extreme points of the feature to in its middle point, achieving the final tubular shape of the ESG stomach. A General Contact (Explicit) was added to prevent interpenetration phenomena amongst the stomach walls during the closing of the wire elements.

The mechanical behaviour of the stomach tissues was defined by means of a fibre-reinforced hyperelastic constitutive formulation, which included the tissue anisotropy and nonlinear elasticity. Both the complete formulation and the procedure for parameters identification (Table 1) are fully reported in previous work [5], and below the constitutive equations are reported in terms of strain energy function W, related to ground matrix W_m and fibre contribution W_f:

$$W^0(\boldsymbol{C}) = W_m^0(\boldsymbol{C}) + W_f^0(\boldsymbol{C}, \boldsymbol{d}_0, \boldsymbol{e}_0) \tag{1}$$

$$W_m^0(\boldsymbol{C}) = \left[\frac{C_1}{\alpha_1}\right]\{\exp[\alpha_1(I_1 - 3)] - 1\} \tag{2}$$

$$\begin{aligned} W_f^0(\boldsymbol{C}, \boldsymbol{d}_0, \boldsymbol{e}_0) \quad = \quad & \frac{C_4}{\alpha_4^2}\{\exp[\alpha_4(I_4 - 1)] - \alpha_4(I_4 - 1) - 1\} \\ & + \frac{C_6}{\alpha_6^2}\{\exp[\alpha_6(I_6 - 1)] - \alpha_6(I_6 - 1) - 1\} \end{aligned} \tag{3}$$

where I_1 is the first of the right Cauchy-Green strain tensor $\boldsymbol{C}$, $\boldsymbol{d_0}$ and $\boldsymbol{e_0}$ define the orientation of collagen (within the connective stratum) or muscular (within the muscularis externa) fibers, while I_4 and I_6 are structural invariants that specify the square of tissue stretch along circumferential and longitudinal directions, respectively. Constitutive parameter C_1 specifies the tissue initial shear stiffness, while parameter α_1 regulates the non-linearity of the shear response. Parameters C_4 and C_6 are constants that define the fibers initial stiffness, while α_4 and α_6 depend on fibers stiffening with stretch.

Hence, to simulate an inflation process mimicking the process of food ingestion, a fluid cavity interaction was defined in the internal region of the stomach (Fig. 1g). Each computational analysis was performed by progressively increasing the intracavity pressure up to 5 kPa during a step time of 1 s, then exploring the effects in the physiological range 0–4 kPa. For ESG models, the first part (up to 0.5 s) of the simulation was dedicated to the wire displacement, and the second part (1 s) to the inflation process, reaching a simulation time of 1.5 s. All the analyses were performed by means of Abaqus Explicit 2020 (Dassault Systemes).

From the computational simulations, the pressure-volume behaviour of each model was extracted. The data points were fitted following the exponential model reported in the Eq. (4), where p_{fit} indicates the pressure vector obtained from the fitting model, V is the vector representing the inflated volume (it starts from 0 up to 1500 ml to describe the highest pre-surgical stomach capacities), a_0 and $b_0$are the fitting parameters that describe the initial slope and the exponential growth of the pressure-volume behaviour, respectively.

$$p_{fit} = a_0 * \left(e^{b_0 * V} - 1\right) \tag{4}$$

3. Results

The computational results are presented in terms of volumetric capacity (pressure–volume response) and distension of gastric wall (elongation stain) for the set of 10 patients on which ESG was simulated and then compared with the pre-surgical and post-LSG configurations.

3.1. Analysis of the gastric reduction

As reported in the introduction, ESG is an endoscopic bariatric procedure that ensures an effective stomach capacity reduction by means of internal sutures, without the removal of gastric tissues, thus contrary to LSG, it preserves the fundus of the stomach. In Table 2, the comparison in terms of volume at different intragastric pressures is proposed for pre- and post-surgical stomach models. On average, ESG recorded a lower reduction of the baseline volume with respect to LSG (56 % and 77 %, respectively), results that are almost mirrored when considering the volumes of inflated stomachs at 4 kPa of intragastric pressure (48 % and 78 %). Significant differences amongst mean volumetric values were recorded between pre- and post-surgical volumes (pre-surgical stomach vs LSG stomach $p = 0.003$ and $p = 0.012$, pre-surgical stomach vs ESG stomach $p = 0.001$ and $p = 0.008$ at baseline and 4 kPa, respectively).

Fig. 5a proposes the pressure-volume behaviour of the pre-surgical, post-LSG and post-ESG stomach models, with a confidential interval of 75 %. The high wideness of the pre-surgical band revealed the

Table 2
Volume comparison in terms of pre- and post-surgical (after simulated ESG and LSG) stomach models at the baseline and at 4 kPa of intragastric pressure.

Patient	Baseline pre-surgical volume [ml]	Baseline post-ESG volume [ml]	Baseline post-LSG volume [ml]	Pre-surgical volume at 4 kPa [ml]	Post-ESG volume at 4 kPa [ml]	Post-LSG volume at 4 kPa [ml]
#A	252.33	111.87	50.19	1265.96	623.38	344.92
#B	327.75	156.81	38.30	2291.39	1309.00	176.90
#C	519.68	196.27	35.28	3400.93	1433.45	216.57
#D	192.47	103.71	56.81	1024.04	708.73	258.83
#E	99.86	45.44	33.89	488.75	302.34	182.08
#F	137.96	63.76	44.71	621.00	342.77	207.26
#G	232.55	108.05	98.36	1250.72	657.20	616.15
#H	112.51	50.23	32.46	691.98	367.10	166.57
#I	112.11	46.24	42.54	551.65	275.88	230.61
#L	130.87	53.38	42.15	500.24	256.40	209.51
Mean (±sd)	211.8 (±131.2)	93.6 (±51.8) $\boldsymbol{p = 0.001}$	47.5 (±19.4) $\boldsymbol{p = 0.003}$	1209 (±948)	628 (±427) $\boldsymbol{p = 0.008}$	261 (±135) $\boldsymbol{p = 0.012}$

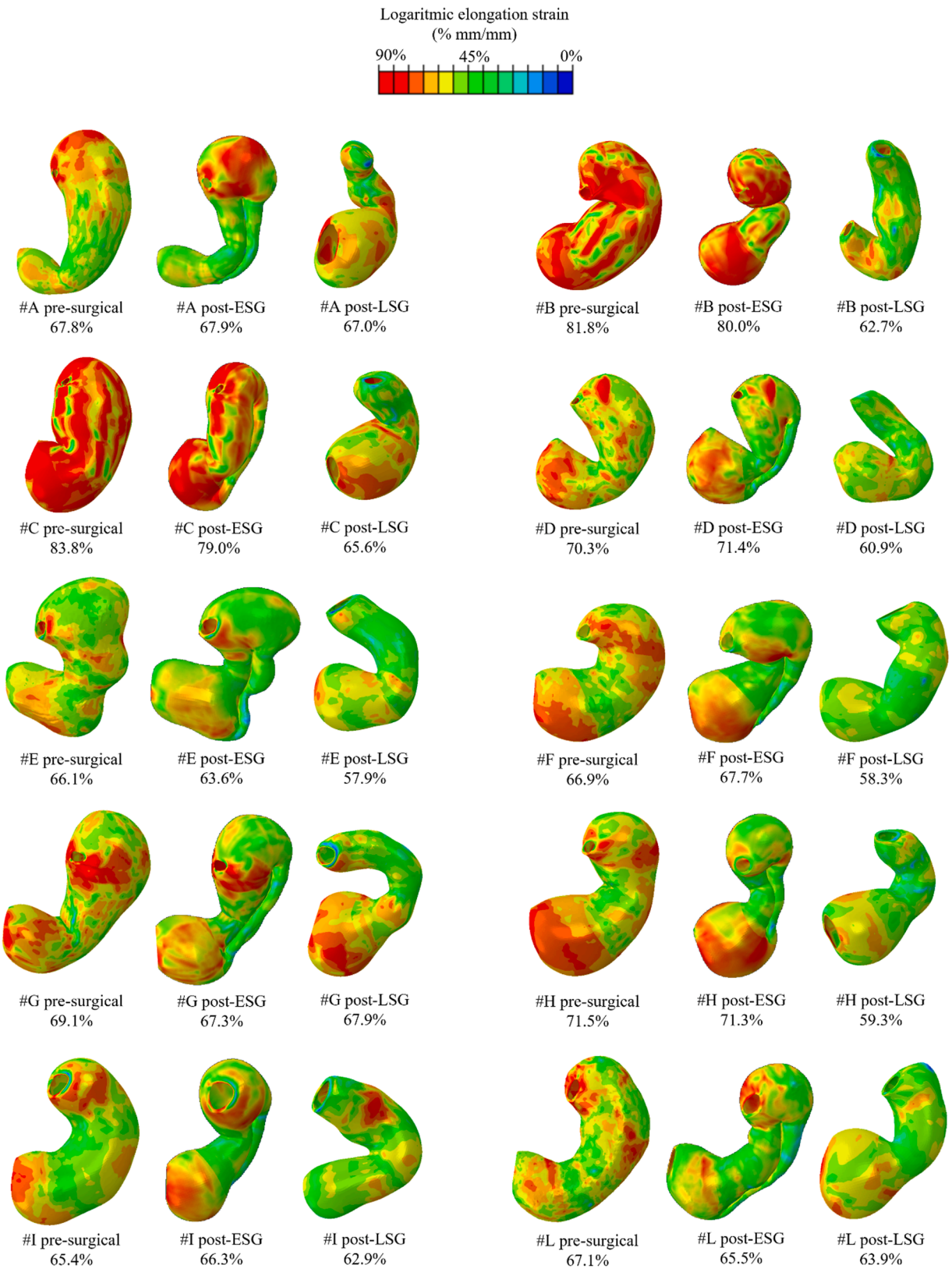

Fig. 2. Elongation strain distribution map in pre- and post-surgical stomachs for an intragastric pressure value of 4 kPa.

pronounced inter-stomach variability in terms of mechanical response, especially for the pre-surgical stomachs and the post-ESG. The pressure-volume bands slightly overlapped, but with clearly different median curves, hence the mechanical response after the inflation process can be considered significantly different amongst the configurations.

3.2. Analysis of the elongation strain

For each of the 10 models, the distribution of ES was exported. The colormaps of these distributions, referring to the gastric wall during the inflation process, are reported in Fig. 2 (not in geometrical scale) when

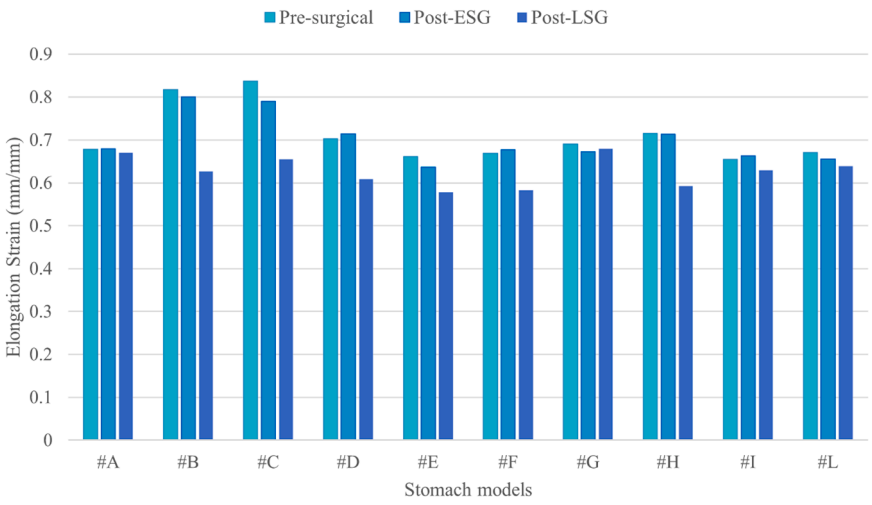

Fig. 3. Comparison of percentage strain values of pre-surgical, post ESG and post LSG models for 4 kPa pressure.

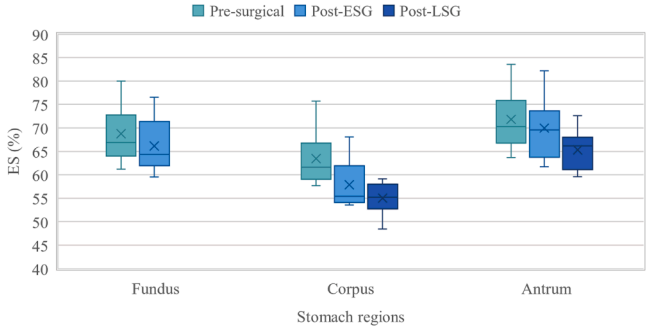

Fig. 4. Comparison of average percentage strain values of pre-surgical, post ESG and post LSG models within the three regions of the stomach (4 kPa of intragastric pressure).

the models reached an inner intragastric pressure of 4 kPa.

In Fig. 3, a comparison of percentage elongation strain values (ES) of pre-, post-ESG, and post-LSG models at different intragastric pressures is reported. Pre-operative models reported an average ES at 4 kPa of intragastric pressure of 71.0 % ± 6.2 %, while lower results were obtained for post-ESG (70.0 % ± 5.3 %) and post-LSG models (62.6 % ± 3.4 %). Significant differences resulted between pre-surgical and post-LSG models ($p < 0.0001$), similarly to [14], while for ESG models no statistical difference was observed with respect to pre-surgical ones ($p = 0.138$).

Details of the ES within the three main regions of the stomach were also extracted from the computational analyses. On average, for post-ESG the greater reduction of the ES was recorded in the corpus region, while post-LSG a general reduction can be observed in both the corpus and antrum regions. On average, at 4 kPa of intragastric pressure, fundus ES was 68.8 % ± 5.8 % in the pre-operative stomachs, while it reduced to 66.1 % ± 5.6 % after ESG. For the corpus, pre-surgical models reported an average ES of 63.5 % ± 6.1 %, while more reduction was achieved both after LSG and ESG (55.0 % ± 3.2 % and 57.9 % ± 5.0 % respectively). Finally, the antrum appeared to be the less altered region, with an average ES of 71.8 % ± 6.4 % in the pre-surgical models, 65.3 ± 4.0 % in the post-LSG and 70.0 % ± 6.2 % in the post-ESG (Fig. 4).

3.3. Data prediction

The pressure-volume data obtained from the simulations were fitted following the exponential model reported in Eq. (4). The fitting parameters (a_0 and b_0) are reported in Table 4 for all the 10 considered patients and for the median curve obtained from the computational analyses (50th percentile) of the three configurations (pre-surgical, post-LSG, and post-ESG configurations).

From the calculation of the parameters a_0 and b_0, a simple predictive model was developed to forecast the resulting pressure-volume relationships after both LSG and ESG for each patient.

The ratios A_{LSG}, A_{ESG}, B_{LSG} and B_{ESG} can be calculated as:

$$A_{LSG}^{(i)} = \frac{a_{0,LSG}^{(i)}}{a_{0,PRE}^{(i)}} \quad 1 \le i \le 10 \tag{5}$$

$$B_{LSG}^{(i)} = \frac{b_{0,LSG}^{(i)}}{b_{0,PRE}^{(i)}} \quad 1 \le i \le 10 \tag{6}$$

$$A_{ESG}^{(i)} = \frac{a_{0,ESG}^{(i)}}{a_{0,PRE}^{(i)}} \quad 1 \le i \le 10 \tag{7}$$

$$B_{ESG}^{(i)} = \frac{b_{0,ESG}^{(i)}}{b_{0,PRE}^{(i)}} \quad 1 \le i \le 10 \tag{8}$$

where i identifies the number of the patient, from 1 to 10 (reported in Table 3). Then the median ratios (A_{LSG}^m, A_{ESG}^m, B_{LSG}^m and B_{ESG}^m) can be obtained as the median of the 10 values for each coefficient.

Then, starting from the pre-surgical pressure-volume behaviour, the estimated post-surgical curve for each patient could be expressed as:

$$p_{LSG}^{(i)} = a_{0,PRE}^{(i)} * A_{LSG}^m * \left(e^{b_{0,PRE}^{(i)} * B_{LSG}^m * V} - 1\right) \tag{9}$$

$$p_{ESG}^{(i)} = a_{0,PRE}^{(i)} * A_{ESG}^m * \left(e^{b_{0,PRE}^{(i)} * B_{ESG}^m * V} - 1\right) \tag{10}$$

The analysis of the discrepancy between the results obtained through computational simulations and the predictive model pointed out an average RMSE of 0.7859 and 0.3614 kPa, for the prediction of LSG and ESG in terms of pressure-volume behaviour, respectively (Table 5). In terms of area of the statistical bands, the difference in percentage recorded amongst the bands calculated through computational pressure-volume data and predictive models was very low for ESG models (the predictive model presented a band 0.5 % less wide than the one obtained with computational results), while the difference was more marked when LSG models were considered. Indeed, the area of the statistical LSG band was 127 % wider than the one obtained from pressure-volume data of LSG simulations.

Table 3
Computational measured elongation strain values for each patient, differentiated in stomach region at an intragastric pressure of 4 kPa.

Patient	Gastric Region	Strain mode of **pre-surgical** stomachs [-]	Strain mode of **post-ESG** stomachs [-]	Strain mode of **post-LSG** stomachs [-]	% Elements respect to the whole model (for **pre-surgical and post-ESG models**)	% Elements respect to the whole model (for **post-LSG models**)
	Fundus	0.61	0.64	-	31.3 %	-
#A	Corpus	0.54	0.48	0.59	53.2 %	45.4 %
	Antrum	0.68	0.57	0.65	15.5 %	54.6 %
	Fundus	0.82	0.70	-	29 %	-
#B	Corpus	0.55	0.57	0.46	48.3 %	67.5 %
	Antrum	0.77	0.88	0.59	22.7 %	32.5 %
	Fundus	0.79	0.71	-	18.1 %	-
#C	Corpus	0.75	0.55	0.45	56.7 %	51.9 %
	Antrum	0.78	0.71	0.60	25.2 %	48.1 %
	Fundus	0.57	0.58	-	26.1 %	-
#D	Corpus	0.58	0.60	0.40	46.1 %	70.5 %
	Antrum	0.67	0.71	0.60	27.8 %	29.5 %
	Fundus	0.53	0.50	-	31 %	-
#E	Corpus	0.64	0.42	0.43	41.9 %	62 %
	Antrum	0.59	0.57	0.60	27.1 %	38 %
	Fundus	0.51	0.55	-	27.1 %	-
#F	Corpus	0.57	0.50	0.41	49.9 %	68.4 %
	Antrum	0.67	0.65	0.56	23 %	31.6 %
	Fundus	0.68	0.56	-	20.4 %	-
#G	Corpus	0.59	0.51	0.55	57.5 %	59 %
	Antrum	0.65	0.69	0.69	22.1 %	41 %
	Fundus	0.64	0.63	-	23.3 %	-
#H	Corpus	0.60	0.51	0.37	43.3 %	56.8 %
	Antrum	0.71	0.71	0.55	33.4 %	43.2 %
	Fundus	0.52	0.69	-	26.3 %	-
#I	Corpus	0.49	0.47	0.49	53.2 %	69.3 %
	Antrum	0.72	0.63	0.51	20.5 %	30.7 %
	Fundus	0.53	0.46	-	21.8 %	-
#L	Corpus	0.50	0.69	0.50	58.6 %	58 %
	Antrum	0.57	0.56	0.59	19.6 %	42 %

4. Discussion

Computational biomechanics has been gaining credibility as a valuable tool to analyse the biological mechanical response of both tissues and organs, and the changes induced by pathologies, medical treatments and surgery. Mechanical stimuli are crucial in regulating normal activities and processes such as tissue remodelling, regeneration or disease, thus their alteration could lead to spoiled organs behaviour and functions.

Concerning the gastrointestinal system, gastric mechano-solicitation is pivotal in the regulation of both satiation during food intake and post-prandial satiety. Several authors demonstrated that distension of the stomach triggers the activation of mechanosensitive receptors that, in turn, relay satiating information to the brain [33,34]. In bariatric surgery, satiety assumes a crucial role in the loosening of short-term weight and in its long-term maintenance, hence proper gastric stimulation is desirable together with a reduction in gastric capacity. However, the quantification of the gastric wall elongation is quite challenging to collect both in vivo and ex vivo. Therefore, in silico models can be a useful tool for quantifying gastric wall stimulation and forecasting post-surgical gastric capacity and strain distribution, especially when referring to patient-specific models.

The computational analyses showed that, for the same patient, LSG and ESG resulted in two different mechanical responses. From Fig. 3 and Table 3, a statistically significant reduction in the elongation strain is shown after LSG, while no differences were observed after ESG when considering the total ES for the models. Contour plots of the stomachs revealed how ESG seemed to recreate the original elongation field along the stomach, with fewer alterations with respect to LSG (Fig. 2). For what concerns the gastric reduction (Table 2), both post-LSG and post-ESG configurations showed a significant volume reduction with respect to the pre-surgical stomach, both at baseline and at 4 kPa, which is supported also by clinical studies [27]. The decreased gastric capacity can be observed also in the pressure-volume curves in Fig. 5.

These results can be traced back to the fact that between LSG and ESG subsists a fundamental difference in the surgical method: LSG and ESG provide a strong capacity reduction of gastric volume, but only LSG implies the almost total removal of the fundus, which is totally preserved after ESG. Moreover, ESG modifies the final stomach configuration only by means of sutures. This affects greatly the final ES pattern, and hence the gastric wall solicitation [35,36]. In fact, the fundus is the softest region of the stomach and acts as a reservoir [5] for these reasons its presence or lack leads to different pressure-volume behaviour and ES values in the post-surgical stomach configurations. The presence of fundus led to more adherence to the pre-surgical configuration in terms of strain distribution, detectable in post-ESG results (Figs. 2 and 4). However, the presence of sutures added several constraints in the corpus, resulting in a stiffer region with a limited extension of the wall. This condition is evident in Fig. 3 and Table 4, where for post-ESG models, the corpus reported the greatest reduction in the ES when comparing with the pre-surgical models, with respect to the other regions (about 90 % of the pre-surgical ES). On the other hand, the lower values in post-LSG models were caused by a series of linked factors, such as the lack of the fundus, the strong tubulisation of the stomach and the consequent decreased in wall tension (Laplace's law).

All these mechanical insights could be useful to understand and prevent many post-operative drawbacks, especially in the long term, as food intolerance and post-operative vomiting after food intake, which are still present at 5 years follow-up [37]. Patient-specific computational clinical tools can address the improper solicitation of the gastric wall due to the modified stomach division in regions and stiffness, through simulating different suture patterns, after-surgical geometrical anatomy and final volumetric capacity, thus identifying the optimal patient-specific surgery design.

Thanks to the predictive model, this study also highlighted an important aspect strictly connected to the surgical procedure. From post-LSG, the resulting variability amongst the models is significantly limited (Fig. 5a), due to the standardisation induced by using a single guide-line tube. On the contrary, pre-operative and post-ESG models resulted in a similar variability, which could be attributed to both the patient- and

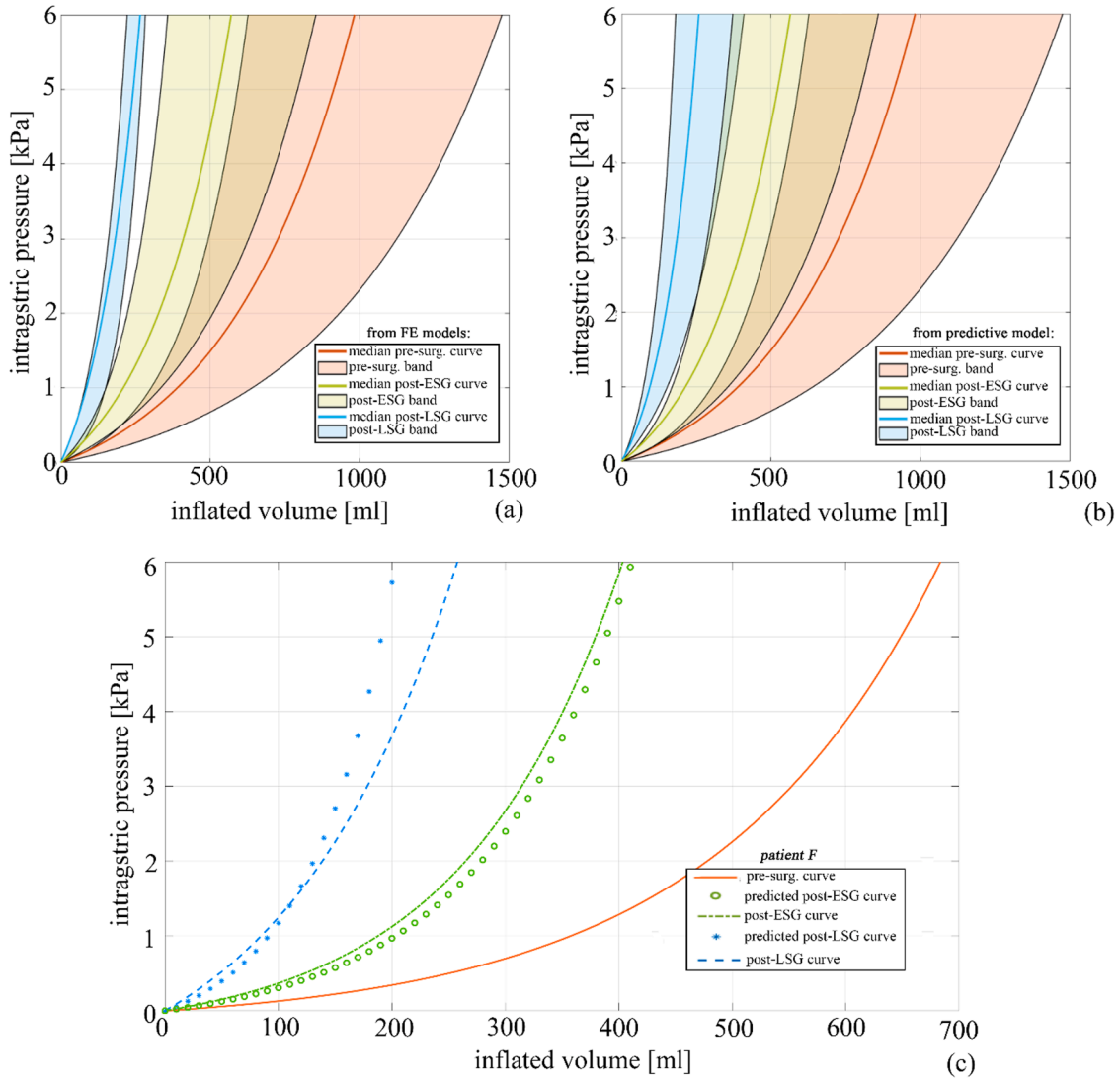

Fig. 5. Pressure-volume behaviour in terms of statistical bands (75 % C.I.) of pre-surgical and post-ESG and post-LSG stomach models obtained from the computational results (a) and with the predictive model Eq. (9) and (10) (b). Comparison between computational results and predictive model for a single patient (#F) (c).

Table 4
Parameters of the model fitting for the pressure-volume curves of pre-surgical, post-LSG and post-ESG stomach models. The ratio is intended as the ratio between the parameter of the post-surgical model (post-LSG and post-ESG) and the corresponding parameter of pre-surgical one.

Patient	a_{0PRE}	b_{0PRE}	a_{0LSG}	b_{0LSG}	a_{0ESG}	b_{0ESG}	A_{LSG}	B_{LSG}	A_{ESG}	B_{ESG}
#A	0.4053	0.0019	1.3590	0.0039	0.5092	0.0034	3.3531	2.0526	1.2564	1.7895
#B	0.5560	0.0009	0.3853	0.0137	1.4477	0.0010	0.6930	14.9531	2.6038	1.0915
#C	0.4634	0.0007	2.1800	0.0047	0.3871	0.0017	4.7044	7.0518	0.8353	2.5506
#D	0.3657	0.0024	0.0855	0.0154	0.7055	0.0026	0.2338	6.4167	1.9292	1.0833
#E	0.2472	0.0058	1.3034	0.0077	0.5403	0.0069	5.2727	1.3276	2.1857	1.1897
#F	0.1971	0.0050	1.3244	0.0066	0.3511	0.0072	6.7194	1.3200	1.7813	1.4400
#G	0.6286	0.0016	1.3690	0.0022	0.6448	0.0029	2.1779	1.3836	1.0258	1.8297
#H	1.2526	0.0021	2.0325	0.0064	1.6864	0.0032	1.6226	3.0476	1.3463	1.5238
#I	0.3215	0.0047	1.3420	0.0059	0.3496	0.0090	4.1742	1.2553	1.2564	1.7895
#L	0.1032	0.0071	1.1357	0.0071	0.1117	0.0141	11.0048	1.0000	2.6038	1.0915
Median curve (50th percentile)	0.7706	0.0022	1.3974	0.0063	0.9112	0.0035	1.8134	2.8636	1.1825	1.5909

surgeon/operator dependence. Within this work, all the post-ESG models were realized by the same operator, but even removing this variable, the patient-dependant stomach anatomy seemed to be the most influencing factor. ESG reduces the final volume of the stomach, but there is no unique standardised procedure, thus the number of stitches, their position and realization could differ from patient to patient. In addition, all the stomachs after LSG should be close to the guide-line tube, thus the percentage of volume reduction between the patients could be different, while for ESG, the percentage of reduction can be similar, but the final volumes could still differ significantly amongst the patients.

Indeed, the predictive model forecasted the post-ESG population, with almost the same confidence intervals and lower RMSE values, while overestimated the post-LSG ones, suggesting that the predictive model

Table 5
Root mean square error (RMSE) between the pressure-volume curve obtained through computational models and the predicted pressure-volume curves obtained through Eq. (9) and (10).

Patients	RMSE between LSG and forecast of LSG for pressure-volume curve [kPa]	RMSE between ESG and forecast of ESG for pressure-volume curve [kPa]
#A	0.0069	0.4542
#B	1.5576	0.0511
#C	2.1117	0.7586
#D	0.0049	0.5416
#E	0.7437	0.1856
#F	0.4060	0.1750
#G	1.3886	0.1926
#H	0.0137	0.0761
#I	1.0574	0.4990
#L	0.5676	0.6800
Mean	0.7859	0.3614

could be a quite simple but effective tool to predict post-operative outcomes when the final result is strongly dependant on the initial configuration rather than forced by the surgical technique (Figs. 5b and 5c).

Being a computational evaluation, this work presents also some limitations that must be considered, due to the high complexity of the problem. These limitations could be seen in the material parameters that describe the mechanical behaviour of the gastric regions (that were obtained on the entire gastric tissues and not on single layers), the boundary conditions that where applied to the gastroesophageal and gastroduodenal junctions, the adoption of a constant intragastric pressure instead of a variable (more physiological) one, the neglect of gastric emptying and the lack of the surrounding organs which could lead to an overestimation of the final volume of the inflated stomach.

However, even if with these simplifications, the reported computational approach has been validated thanks to experimental comparison with clinical data in a previous work by the authors [14], thus supporting both the adopted assumptions and the results obtained within this work.

5. Conclusions

LSG is the most popular bariatric surgery, providing effective weight loss and comorbidity improvement, but also with non-negligible side effects. With the progress of technology, less invasive endoscopic alternatives such as ESG have been proposed, whose initial purpose is to obtain the same results in terms of efficacy together with fewer complications.

Within this framework, this work reported for the first time the computational evaluation and comparison of both techniques with a patient-specific approach, which resulted in different behaviour of the stomach in the post-operative condition, depending on the surgery and the stomach conformation. From the one hand, LSG could provide the patient with a greater reduction in the stomach volume, which would result in consequent rapid weight loss and improvement of comorbidities also in the short term. However, mechanical strains of the gastric cavity would result in an alteration of the satiety process. On the other hand, within the same patient, ESG would replicate a more similar pre-operative situation, in which the gastric wall distension should be almost unaltered and thus the mechanosensation and the regulation of satiation. ESG has been demonstrated to be applicable to every class of obesity; thus in patients declining or unsuitable for surgery, ESG could be considered as an alternative treatment option, revealing its potential for a wide field of application. In addition, the predictive model proposed in this work could support the surgical planning and the estimation of the volume reduction after ESG.

Statements and declarations

Statement of ethics: No ethics approval was required because the study is a further computational elaboration starting from already-published human sensible data.

Ethical review board

Not present.

Funding

This work was supported by MIUR, FISR 2019, Project n FISR2019_03221, titled CECOMES "CEntro di studi sperimentali e COmputazionali per la ModElliStica applicata alla chirurgia" and by the Department of Civil, Environmental and Architectural Engineering, University of Padova, BIRD2022 “Computational gastric biomechanics to improve bariatric surgery procedures with a patient-specific approach”.

CRediT authorship contribution statement

Ilaria Toniolo: Conceptualization, Methodology, Software, Validation, Investigation, Data curation, Writing – original draft, Writing – review & editing. **Paola Pirini:** Methodology, Software, Investigation, Data curation, Writing – review & editing. **Silvana Perretta:** Resources, Writing – review & editing. **Emanuele Luigi Carniel:** Resources, Writing – review & editing, Funding acquisition. **Alice Berardo:** Conceptualization, Methodology, Software, Validation, Investigation, Data curation, Writing – original draft, Writing – review & editing, Supervision, Funding acquisition.

Declaration of Competing Interest

The authors declare that they have no conflict of interest.

Acknowledgments

The authors would like to thank Dr. Damiano Remor for his consulting and advice.

References

[1] H.B. Henninger, S.P. Reese, A.E. Anderson, J.A. Weiss, Validation of computational models in biomechanics, Proc. Inst. Mech. Eng. Part H J. Eng. Med. 224 (2010) 801–812, https://doi.org/10.1243/09544119JEIM649.
[2] K. Miller, G.R. Joldes, G. Bourantas, S.K. Warfield, D.E. Hyde, R. Kikinis, A. Wittek, Biomechanical modeling and computer simulation of the brain during neurosurgery, Int. j. Numer. Method. Biomed. Eng. 35 (2019) 1–24, https://doi.org/10.1002/cnm.3250.
[3] G. Biglino, C. Capelli, J. Bruse, G.M. Bosi, A.M. Taylor, S. Schievano, Computational modelling for congenital heart disease: how far are we from clinical translation? Heart 103 (2017) 98–103, https://doi.org/10.1136/heartjnl-2016-310423.
[4] M. Peirlinck, F.S. Costabal, J. Yao, J.M. Guccione, S. Tripathy, Y. Wang, D. Ozturk, P. Segars, T.M. Morrison, S. Levine, E. Kuhl, Precision medicine in human heart modeling: perspectives, challenges, and opportunities, Biomech. Model. Mechanobiol. 20 (2021) 803–831, https://doi.org/10.1007/s10237-021-01421-z.
[5] I. Toniolo, C.G. Fontanella, M. Foletto, E.L. Carniel, Coupled experimental and computational approach to stomach biomechanics: towards a validated characterization of gastric tissues mechanical properties, J. Mech. Behav. Biomed. Mater. 125 (2021), 104914, https://doi.org/10.1016/j.jmbbm.2021.104914.
[6] J. Zhao, D. Liao, P. Chen, P. Kunwald, H. Gregersen, Stomach stress and strain depend on location, direction and the layered structure, J. Biomech. 41 (2008), 3441–3447–3441–3447.
[7] M.V. Mascolini, C.G. Fontanella, A. Berardo, E.L. Carniel, Influence of transurethral catheters on urine pressure-flow relationships in males : a computational fluid-dynamics study, Comput. Methods Programs Biomed. 238 (2023) 9–12, https://doi.org/10.1016/j.cmpb.2023.107594.
[8] A.G. Hannam, Current computational modelling trends in craniomandibular biomechanics and their clinical implications, J. Oral Rehabil. 38 (2011) 217–234, https://doi.org/10.1111/j.1365-2842.2010.02149.x.

[9] L. Shu, S. Li, N. Sugita, Systematic review of computational modelling for biomechanics analysis of total knee replacement, Biosurface and Biotribology 6 (2020) 3–11, https://doi.org/10.1049/bsbt.2019.0012.
[10] A. Arduino, S. Pettenuzzo, A. Berardo, V.A. Salomoni, C. Majorana, E.L. Carniel, A continuum-tensegrity computational model for chondrocyte biomechanics in afm indentation and micropipette aspiration, Ann. Biomed. Eng (2022), https://doi.org/10.1007/s10439-022-03011-1.
[11] I. Toniolo, C. Salmaso, G. Bruno, A. De Stefani, C. Stefanini, A.L.T. Gracco, E. L. Carniel, Anisotropic computational modelling of bony structures from CT data: an almost automatic procedure, Comput. Methods Programs Biomed. 189 (2020), https://doi.org/10.1016/j.cmpb.2020.105319.
[12] A. Pretto, I. Toniolo, A. Berardo, G. Savio, S. Perretta, E.L. Carniel, F. Uccheddu, Automatic segmentation of stomach of patients affected by obesity, in: 2023: pp. 276–285. 10.1007/978-3-031-15928-2_24.
[13] X. Xu, C. Liu, Y. Zheng, 3D tooth segmentation and labeling using deep convolutional neural networks, IEEE Trans. Vis. Comput. Graph. 25 (2019) 2336–2348, https://doi.org/10.1109/TVCG.2018.2839685.
[14] I. Toniolo, A. Berardo, M. Foletto, C. Fiorillo, G. Quero, S. Perretta, E.L. Carniel, Patient-specific stomach biomechanics before and after laparoscopic sleeve gastrectomy, Surg. Endosc. (2022), https://doi.org/10.1007/s00464-022-09233-7.
[15] S. Avril, M.W. Gee, A. Hemmler, S. Rugonyi, Patient-specific computational modeling of endovascular aneurysm repair: state of the art and future directions, Int. j. Numer. Method. Biomed. Eng. 37 (2021) 1–19, https://doi.org/10.1002/cnm.3529.
[16] R.A. Gray, P. Pathmanathan, Patient-specific cardiovascular computational modeling: diversity of personalization and challenges, J. Cardiovasc. Transl. Res. 11 (2018) 80–88, https://doi.org/10.1007/s12265-018-9792-2.
[17] M. Sensale, T. Vendeuvre, C. Schilling, T. Grupp, M. Rochette, E. Dall'Ara, Patient-specific finite element models of posterior pedicle screw fixation: effect of screw's size and geometry, Front. Bioeng. Biotechnol. 9 (2021), 643154, https://doi.org/10.3389/fbioe.2021.643154.
[18] C.M. Charlebois, D.J. Caldwell, S.M. Rampersad, A.P. Janson, J.G. Ojemann, D. H. Brooks, R.S. MacLeod, C.R. Butson, A.D. Dorval, Validating patient-specific finite element models of direct electrocortical stimulation, Front. Neurosci. 15 (2021), 691701, https://doi.org/10.3389/fnins.2021.691701.
[19] P.O. Bolcos, M.E. Mononen, K.E. Roach, M.S. Tanaka, J.S. Suomalainen, S. Mikkonen, M.J. Nissi, J. Töyräs, T.M. Link, R.B. Souza, S. Majumdar, C.B. Ma, X. Li, R.K. Korhonen, Subject-specific biomechanical analysis to estimate locations susceptible to osteoarthritis-Finite element modeling and MRI follow-up of ACL reconstructed patients, J. Orthop. Res. Off. Publ. Orthop. Res. Soc. 40 (2022) 1744–1755, https://doi.org/10.1002/jor.25218.
[20] I. Toniolo, A. Berardo, M. Gagner, M. Foletto, E.L. Carniel, Unveiling the effects of key factors in enhancing gastroesophageal reflux: a fluid-structure analysis before and after laparoscopic sleeve gastrectomy, Comput. Methods Programs Biomed. 231 (2023), 107409, https://doi.org/10.1016/j.cmpb.2023.107409.
[21] D.H. Liao, J.B. Zhao, H. Gregersen, Gastrointestinal tract modelling in health and disease, World J. Gastroenterol. 15 (2009), 169–176–169–176.
[22] I. Toniolo, C.G. Fontanella, M. Gagner, C. Stefanini, M. Foletto, E.L. Carniel, Computational evaluation of laparoscopic sleeve gastrectomy, Updates Surg 10 (2021), https://doi.org/10.1007/s13304-021-01046-y.
[23] C.G. Fontanella, C. Salmaso, I. Toniolo, N. de Cesare, A. Rubini, G.M. De Benedictis, E.L. Carniel, Computational models for the mechanical investigation of stomach tissues and structure, Ann. Biomed. Eng (2019) 47, https://doi.org/10.1007/s10439-019-02229-w.
[24] V.O. Brunaldi, M.G. Neto, Y. Ji, Endoscopic sleeve gastroplasty: a narrative review on historical evolution, physiology, outcomes, and future standpoints, Chin. Med. J. (Engl). 135 (2022) 774–778, https://doi.org/10.1097/CM9.0000000000002098.
[25] A. Hedjoudje, B.K. Abu Dayyeh, L.J. Cheskin, A. Adam, M.G. Neto, D. Badurdeen, J.G. Morales, A. Sartoretto, G.L. Nava, E. Vargas, Z. Sui, L. Fayad, J. Farha, M. A. Khashab, A.N. Kalloo, A.R. Alqahtani, C.C. Thompson, V. Kumbhari, Efficacy and safety of endoscopic sleeve gastroplasty: a systematic review and meta-analysis, Clin. Gastroenterol. Hepatol 18 (2020) 1043–1053, https://doi.org/10.1016/j.cgh.2019.08.022, e4.
[26] W.A. Brown, L. Kow, S. Shikora, R. Liem, R. Welbourn, J. Dixon, P. Walton, R. Kinsman, The IFSO global registry IFSO global registry report, 2021.
[27] C. Fiorillo, G. Quero, M. Vix, L. Guerriero, M. Pizzicannella, A. Lapergola, A. D'Urso, L. Swanstrom, D. Mutter, B. Dallemagne, S. Perretta, 6-Month gastrointestinal quality of life (QoL) results after endoscopic sleeve gastroplasty and laparoscopic sleeve gastrectomy: a propensity score analysis, Obes. Surg. 30 (2020) 1944–1951, https://doi.org/10.1007/s11695-020-04419-1.
[28] J.W. Wang, C.Y. Chen, Current status of endoscopic sleeve gastroplasty: an opinion review, World J. Gastroenterol. 26 (2020) 1107–1112, https://doi.org/10.3748/wjg.v26.i11.1107.
[29] G. Quero, C. Fiorillo, B. Dallemagne, P. Mascagni, J. Curcic, M. Fox, S. Perretta, The causes of gastroesophageal reflux after laparoscopic sleeve gastrectomy: quantitative assessment of the structure and function of the esophagogastric junction by magnetic resonance imaging and high-resolution manometry, Obes. Surg. 30 (2020) 2108–2117, https://doi.org/10.1007/s11695-020-04438-y.
[30] M. MacGinnis, H. Chu, G. Youssef, K.W. Wu, A.W. Machado, W. Moon, The effects of micro-implant assisted rapid palatal expansion (MARPE) on the nasomaxillary complex—A finite element method (FEM) analysis, Prog. Orthod. 15 (2014) 52, https://doi.org/10.1186/s40510-014-0052-y.
[31] A. Sartoretto, Z. Sui, C. Hill, M. Dunlap, A.R. Rivera, M.A. Khashab, A.N. Kalloo, L. Fayad, L.J. Cheskin, G. Marinos, E. Wilson, V. Kumbhari, Endoscopic sleeve gastroplasty (ESG) is a reproducible and effective endoscopic bariatric therapy suitable for widespread clinical adoption: a large, international multicenter study, Obes. Surg. 28 (2018), 1812–1821–1812–1821.
[32] E. Espinet-Coll, J. Nebreda-Durán, M. Galvao-Neto, C. Bautista-Altamirano, P. Diaz-Galán, J.A. Gómez-Valero, C. Vila-Lolo, M.A. Guirola-Puche, A. Fernández-Huélamo, D. Bargalló-Carulla, A. Juan-Creix Comamala, Suture pattern does not influence outcomes of endoscopic sleeve gastroplasty in obese patients, Endosc. Int. Open. 08 (2020) E1349–E1358, https://doi.org/10.1055/a-1221-9835.
[33] P. Janssen, P. Vanden Berghe, S. Verschueren, A. Lehmann, I. Depoortere, J. Tack, Review article: the role of gastric motility in the control of food intake, Aliment. Pharmacol. Ther. 33 (2011), 880–894–880–894.
[34] H. Piessevaux, J. Tack, A. Wilmer, B. Coulie, A. Geubel, J. Janssens, Perception of changes in wall tension of the proximal stomach in humans, Gut 49 (2001), 203–208–203–208.
[35] T.H. Moran, Gastrointestinal signals: satiety, Encycl. Neurosci. (2010), 571–576–571–576.
[36] A. Kretschmer, T. Hüsch, F. Thomsen, D. Kronlachner, T. Pottek, A. Obaje, R. Anding, A. Rose, R. Olianas, A. Friedl, W. Hübner, R. Homberg, J. Pfitzenmaier, U. Grein, F. Queissert, C.M. Naumann, J. Schweiger, C. Wotzka, J.N. Nyarangi-Dix, T. Hofmann, A. Buchner, A. Haferkamp, R.M. Bauer, Debates on male incontinence (DOMINO)-project, efficacy and safety of the zsi375 artificial urinary sphincter for male stress urinary incontinence: lessons learned, World J. Urol. 34 (2016) 1457–1463, https://doi.org/10.1007/s00345-016-1787-5.
[37] P. Małczak, M. Mizera, Y. Lee, M. Pisarska-Adamczyk, M. Wysocki, M.M. Bała, J. Witowski, M. Rubinkiewicz, A. Dudek, T. Stefura, G. Torbicz, P. Tylec, N. Gajewska, T. Vongsurbchart, M. Su, P. Major, M. Pędziwiatr, Quality of life after bariatric surgery—A systematic review with bayesian network meta-analysis, Obes. Surg. 31 (2021) 5213–5223, https://doi.org/10.1007/s11695-021-05687-1.